

Supporting Information for “Temperature-induced nonlinear elastic behavior in Berea sandstone explained by a modified sheared contacts model”

Jonathan Simpson^{1,2}, Kasper van Wijk^{1,2}, Ludmila Adam^{2,3}, and Lionel Esteban⁴

¹Physical Acoustics Laboratory, Department of Physics, University of Auckland, Auckland, New Zealand

²Dodd-Walls Centre for Photonic and Quantum Technologies, Auckland, New Zealand

³Physics of Rocks Laboratory, Department of Physics, University of Auckland, Auckland, New Zealand

⁴CSIRO-Energy, Perth, Western Australia, Australia

Contents of this file

1. Figures S1 to S2
2. Section S1: Details of XRD Methodology
3. Section S2: Temperature Diffusion Modeling of the Berea Sandstone Sample

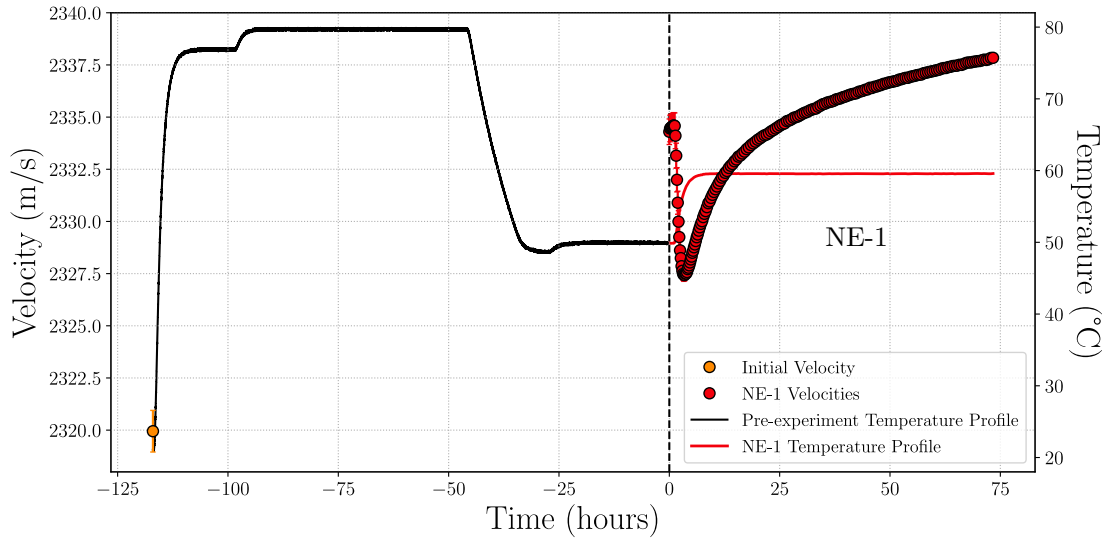


Figure S1. Plot showing the velocity and temperature evolution of the Berea sandstone sample before the first nonlinear experiment (NE-1) started. The orange point shows the ultrasonic velocity measured at room temperature before the temperature of the pressure vessel was increased. The temperature was then increased to 80°C and held constant for ~60 hours, before being reduced to 50°C and held constant for ~30 hours. This ensured that any residual humidity was removed. The data in red shows the temperature and measured velocity during NE-1 for reference, and is identical to that presented in Figure 3(a). Time is measured in hours from the beginning of NE-1 (indicated by the vertical dashed line). A vacuum was continuously maintained in the pressure vessel during this entire period.

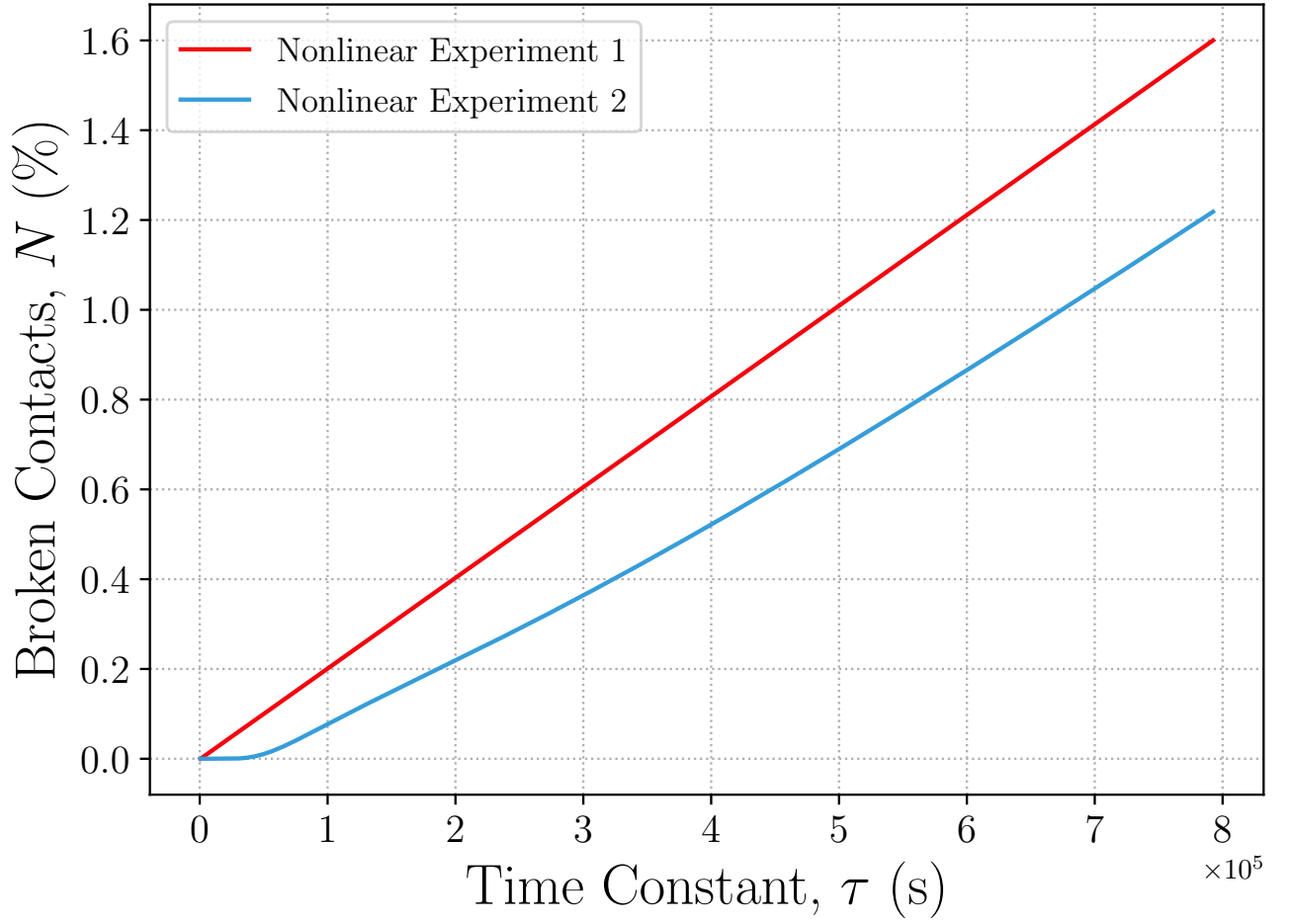


Figure S2. Initial profiles of broken contacts as a function of time constant τ for the two models in Figure 5. A linear profile was chosen for the first experiment (red), ranging from 0 broken contacts for τ_{min} to $c = 1.6\%$ broken contacts for τ_{max} . For Nonlinear Experiment 2, we used the final profile of the model from Nonlinear Experiment 1 as the initial profile for τ .

S1: Details of XRD Methodology

Mineral volume percentages of the Berea sandstone sample were estimated using X-ray diffraction (XRD) analysis. XRD patterns were recorded with a PANalytical X'Pert Pro Multi-purpose Diffractometer using Fe filtered Co K α radiation, an automatic divergence slit, a 2° anti-scatter slit, and a fast X'Celerator Si strip detector. The diffraction patterns were recorded from 3 to 80° in steps of 0.017° 2-theta with a 0.5 second counting time per step for an overall counting time of approximately 35 minutes. Qualitative analysis was performed on the XRD data using in-house XPLOT and HighScore Plus (from PANalytical) search/match software. Quantitative analysis was performed on the XRD data using the commercial package TOPAS from Bruker AXT. The results are normalized to 100%, and hence do not include estimates of unidentified or amorphous materials. The final percentage volume of minerals are as follows; quartz and plagioclase, 84%; kaolinite, 2.2%; mica/illite, 2.3%; dolomite, 3.8%; microcline, 5%; others, 2.7%.

S2: Temperature Diffusion Modeling of the Berea Sandstone Sample

In this section, we present the results of a numerical model to understand how the temperature of the Berea sandstone sample corresponds to the temperature measured with the thermocouple inside the pressure vessel. These results will allow us to determine if any temperature difference between the sample and the measured values may influence the velocity changes we observe.

To model the temperature of the sample, we use COMSOL Multiphysics® finite element software (COMSOL AB, 2022). A 3-dimensional computer-assisted design model of the apparatus is imported into the software to serve as the geometry of the model (Figure S3a). This geometry includes the pressure vessel, the sample holder and its stand, and the Berea sandstone sample. All dimensions are representative of the actual experimental apparatus. Each component of the geometry is assigned relevant material properties, as listed in Table S1. We run the model with several different values for the material properties of the Berea sample to cover the range of reasonable values quoted in the literature. We also choose a set of conservative values that represent the “worst-case” scenario for thermal conduction and diffusion in the Berea sample.

For the physics of our model, only heating by thermal conduction could be calculated. This means that the only source of heating (or cooling) for the Berea sample is through contact with the sample holder. In reality, heating and cooling would also occur through thermal radiation inside the pressure vessel, meaning that our models will represent overestimates of the difference between the measured and actual temperature of the sample. Due to the vacuum inside the vessel, heating by convection or conduction through air is not considered. The equation governing the physics in the model is:

$$\rho C \frac{\partial T}{\partial t} + \nabla \cdot (-k \nabla T) = Q, \quad (1)$$

where ρ is the density, C is the specific heat capacity, T is temperature, k is thermal conductivity, t is time, and Q contains external heat sources (with units of W m^{-3}). This equation is implemented using a finite element analysis with a fine mesh in time-dependent heat transfer studies for both heating and cooling between 50 and 60°C. In our experiments, the external heat flux is provided by the heating mantle on the outside of the pressure vessel. However, since we do not measure the flux directly, we instead provide the model with two temperature boundary conditions. The boundary conditions at each time step are defined using the temperatures we record during the experiment on the external wall of the pressure vessel (denoted “External Temperature” in Figures S4 and S5) and via the thermocouple inside the thermowell (denoted “Internal Temperature” in Figures S4 and S5). Although we do not model the thermowell in the geometry, we set the temperature of the inner walls of the pressure vessel to the temperature recorded by this thermocouple. The starting temperature of the sample holder and Berea sample are set to the initial equilibrium temperatures for each experiment. The number and size of the time steps are variable and determined by the solver, with steps as small as 1 s or as large as 1000 s for periods of large and small temperature changes, respectively.

Table S1. Values of the material properties used in the model. Multiple values are given for some of the Berea parameters, as different values were used to build a range of models.

Component:	Vessel and holder post	Sample holder	Sample
Material:	Stainless Steel 316	Aluminum	Berea sandstone
Density, ρ (kg m^{-3})	8000	2700	2100 ^a
Specific heat capacity, C ($\text{J kg}^{-1}\text{K}^{-1}$)	500	900	960 ^b , 1200 ^c
Thermal conductivity, k ($\text{W m}^{-1}\text{K}^{-1}$)	16.3	238	2.0 ^c , 3.5 ^b
Thermal diffusivity ^d , α ($\times 10^{-7} \text{ m}^2 \text{ s}^{-1}$)	40.8	979	7.9, 9.9, 17.4

^aCalculated from the dimensions and mass of sample

^bBest estimate for Berea sandstone under our conditions from Robertson (1988)

^cA conservative maximum/minimum value based on ranges for common rocks in Robertson (1988)

^dCalculated using $\alpha = k/(\rho \cdot C)$

Figures S3 through S5 show results of two models: one using the most conservative parameters for the Berea sandstone ($C = 1200 \text{ J kg}^{-1}\text{K}^{-1}$, $k = 2.0 \text{ W m}^{-1}\text{K}^{-1}$, and $\alpha = 7.9 \times 10^{-7} \text{ m}^2 \text{ s}^{-1}$), and the other using our “best estimate” for the parameters, reflecting more typical values for Berea sandstone ($C = 960 \text{ J kg}^{-1}\text{K}^{-1}$, $k = 3.5 \text{ W m}^{-1}\text{K}^{-1}$, and $\alpha = 17.4 \times 10^{-7} \text{ m}^2 \text{ s}^{-1}$). For both heating and cooling, the temperature of the Berea sample lags behind the recorded internal temperature. This is due to the time needed for heat to be conducted and diffused into the Berea sample via the sample holder. The maximum temperature difference between the recorded

temperature and the center of the sample for the conservative model is no more than 1.4°C for heating and 0.8°C for cooling. For the best estimate model, the differences are even less (0.8°C and 0.6°C , respectively). We also note that the center temperature of the sample lags behind the recorded internal pressure vessel temperature by 25 minutes at most. The results of the model also clearly show that there is very little temperature variation within the Berea sample itself; the profiles for the temperature at the center of the sample and the temperature at the edge of the sample are near identical at all times. This confirms that heat diffuses within the sample much faster than the smallest time interval (10 minutes) between waveform acquisitions in our experiments. The temperature at the edge is very slightly less than the temperature at the center because the edge temperature is measured at the top of the sample (i.e. at the point furthest from the location of heat conduction).

Our modeling shows that the temperature profile of the Berea sandstone sample closely follows the temperature we record within the pressure vessel during our experiments, and that the temperature is essentially uniform throughout the sample at all times. Considering that these models do not account for heating and cooling by thermal radiation, the actual variation between the recorded internal temperature and the sample will be even smaller than what is presented here. This gives us confidence that the measured temperature within the pressure vessel is an accurate representation of the temperature of the sample.

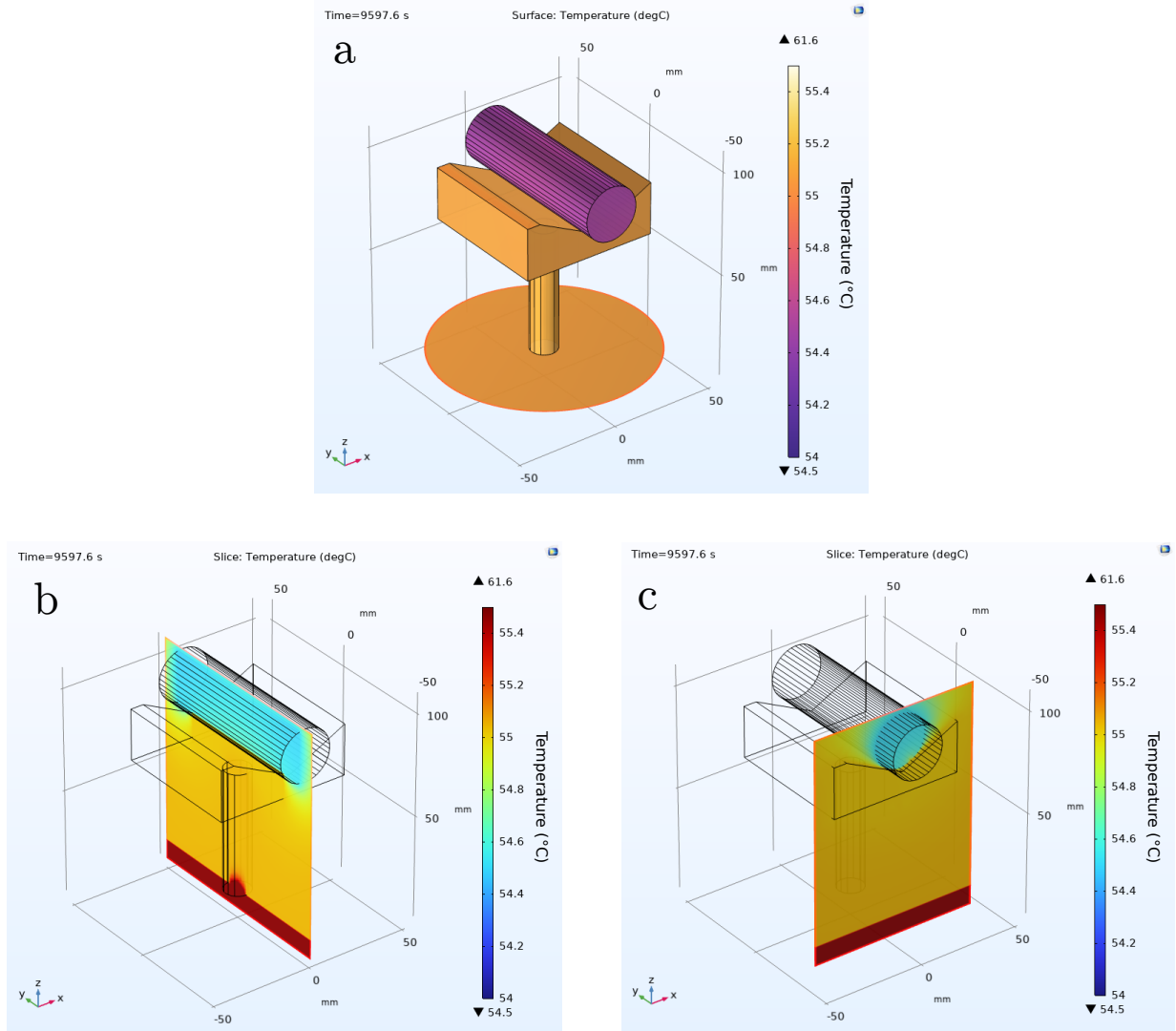


Figure S3. Temperature diffusion model geometry and example results. Panel (a) shows the geometry of the sample in its holder inside the pressure vessel. Note that the pressure vessel is not shown. The colors indicate the surface temperatures at a time step of 9597.6 s (2.66 hr) for a temperature increase. This time is near to the peak temperature gradient. Panel (b) and (c): Cross sections in the y - z and x - z planes, respectively, showing the temperature profiles at the same time as in (a). The dark red strip at the bottom of each cross section corresponds to the bottom pressure vessel wall.

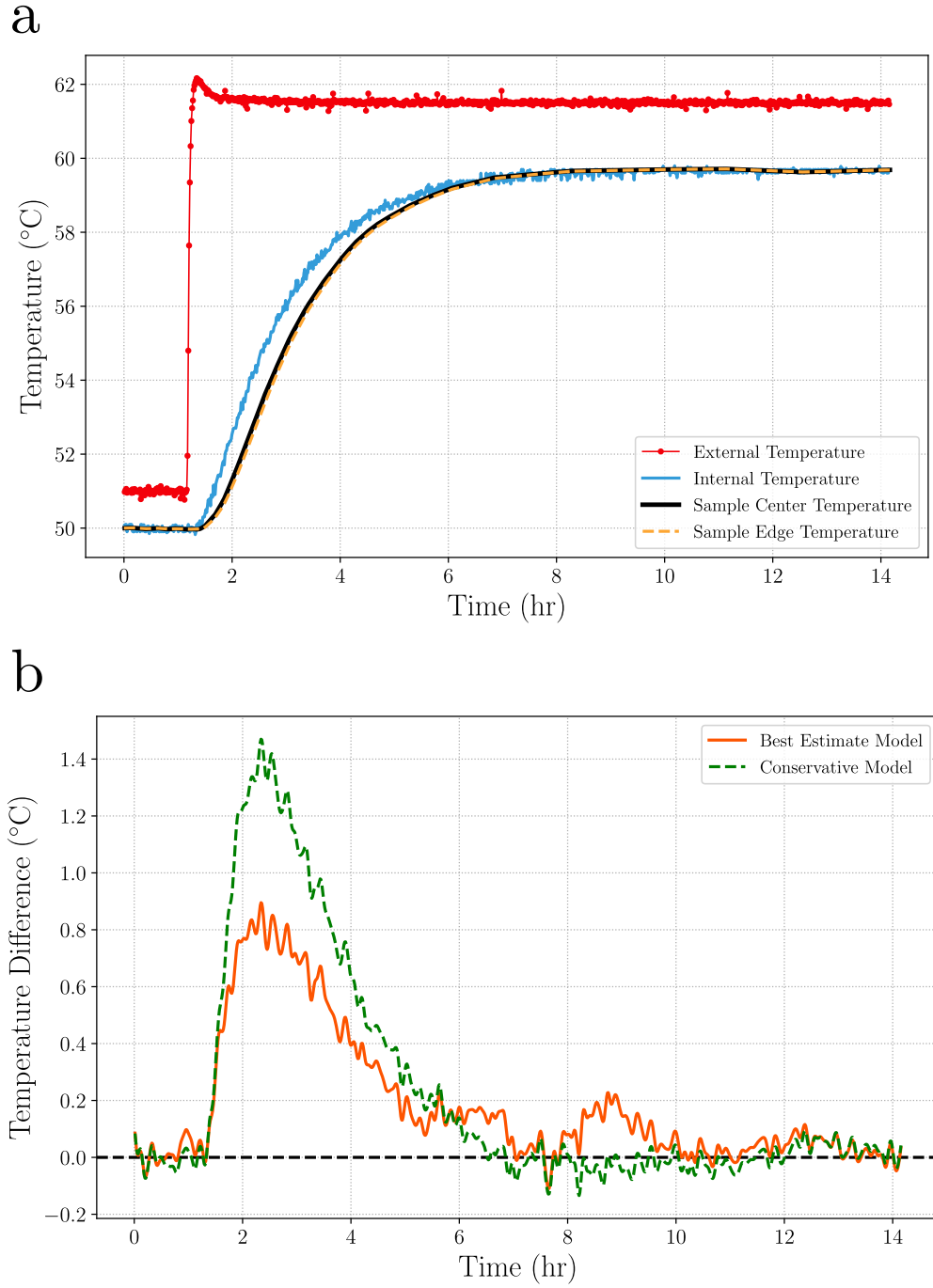


Figure S4. Comparison between measured and modeled temperatures for a temperature increase. Panel (a) shows the temperatures as a function of time for the model using the most conservative values for the material properties of Berea sandstone ($C = 1200 \text{ J kg}^{-1}\text{K}^{-1}$, $k = 2.0 \text{ W m}^{-1}\text{K}^{-1}$, $\alpha = 7.9 \times 10^{-7} \text{ m}^2 \text{ s}^{-1}$). “External Temperature” and “Internal Temperature” refer to the temperatures measured outside and inside the pressure vessel during the experiment, respectively. Panel (b) shows the temperature difference between the measured internal pressure vessel temperature and the center of the sample for both the conservative model and the best estimate model ($C = 960 \text{ J kg}^{-1}\text{K}^{-1}$, $k = 3.5 \text{ W m}^{-1}\text{K}^{-1}$, $\alpha = 17.4 \times 10^{-7} \text{ m}^2 \text{ s}^{-1}$). Note that the variability from equilibrium observed after ~ 8 hours is within the error of the temperature measurements.

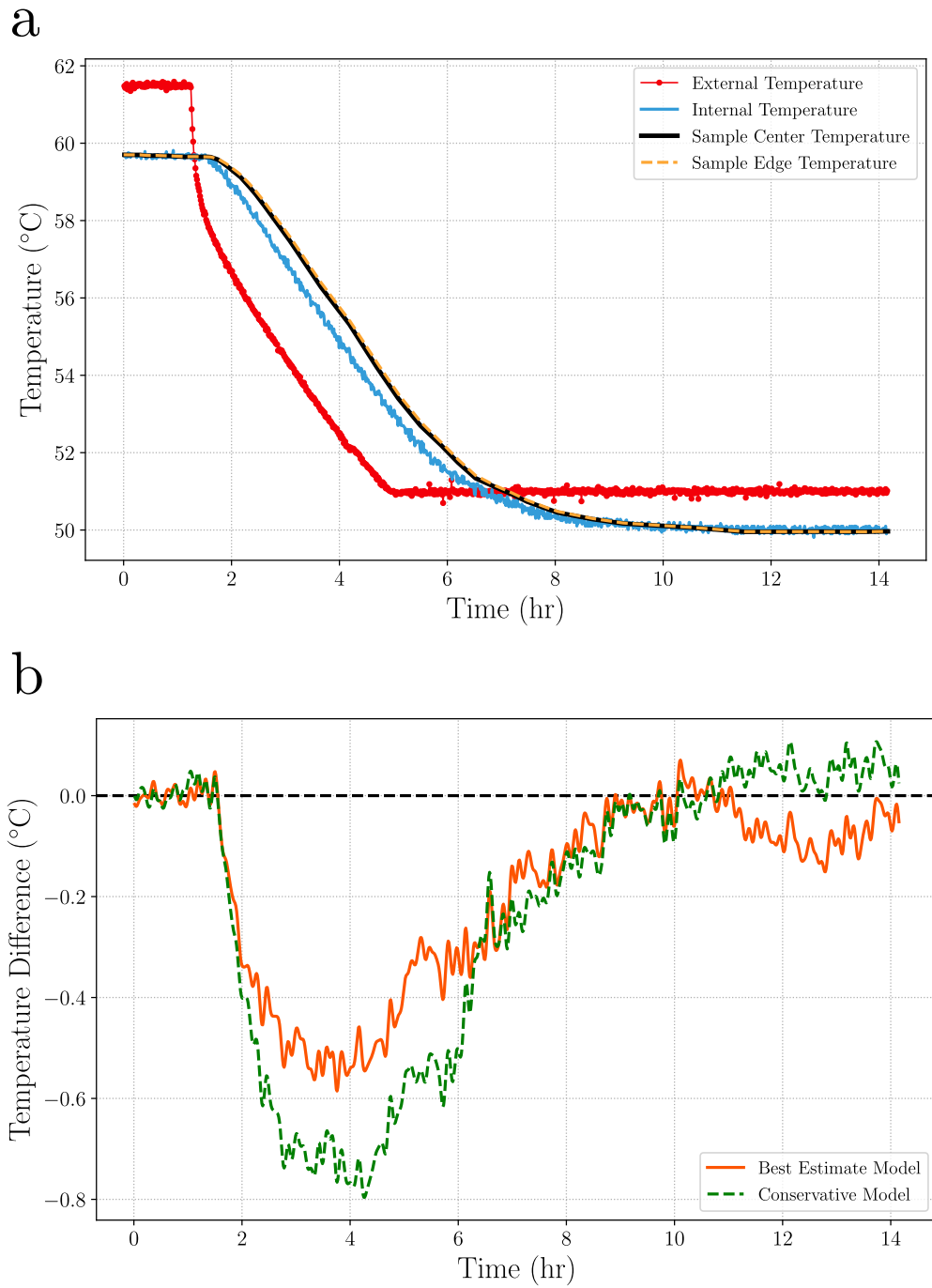


Figure S5. Same as Figure S4, but for a temperature decrease.

References

- COMSOL AB. (2022). *COMSOL Multiphysics® v. 6.1*. www.comsol.com.
- Robertson, E. C. (1988). *Thermal Properties of Rocks* (Tech. Rep.). Reston, VA: US Department of the Interior: Geological Survey.